nature genetics

Exome sequencing identifies truncating mutations in *PRRT2* that cause paroxysmal kinesigenic dyskinesia

Wan-Jin Chen[1,2], Yu Lin[2], Zhi-Qi Xiong[3], Wei Wei[2], Wang Ni[1,2], Guo-He Tan[3], Shun-Ling Guo[3], Jin He[2], Ya-Fang Chen[2], Qi-Jie Zhang[2], Hong-Fu Li[1], Yi Lin[2], Shen-Xing Murong[2], Jianfeng Xu[4,5], Ning Wang[2] & Zhi-Ying Wu[1]

Paroxysmal kinesigenic dyskinesia is the most common type of paroxysmal movement disorder and is often misdiagnosed clinically as epilepsy. Using whole-exome sequencing followed by Sanger sequencing, we identified three truncating mutations within *PRRT2* (NM_145239.2) in eight Han Chinese families with histories of paroxysmal kinesigenic dyskinesia: c.514_517delTCTG (p.Ser172Argfs*3) in one family, c.649dupC (p.Arg217Profs*8) in six families and c.972delA (p.Val325Serfs*12) in one family. These truncating mutations co-segregated exactly with the disease in these families and were not observed in 1,000 control subjects of matched ancestry. *PRRT2* is a newly discovered gene consisting of four exons encoding the proline-rich transmembrane protein 2, which encompasses 340 amino acids and contains two predicted transmembrane domains. *PRRT2* is highly expressed in the developing nervous system, and a truncating mutation alters the subcellular localization of the PRRT2 protein. The function of *PRRT2* and its role in paroxysmal kinesigenic dyskinesia should be further investigated.

Paroxysmal kinesigenic dyskinesia (OMIM 128200) was first described in 1967 and is now recognized as the most common type of paroxysmal movement disorder[1]. Although the exact prevalence is unknown[2], it is estimated at 1 in 150,000 individuals (see URLs). Paroxysmal kinesigenic dyskinesia is characterized by recurrent, brief attacks of dyskinesia that are triggered by sudden voluntary movement[3]. These attacks usually occur during childhood or early adulthood and can involve dystonic postures, chorea or athetosis, manifestations that typically last less than 1 min but can occasionally occur for up to 5 min. Symptoms become less severe with age, and affected individuals respond well to anticonvulsant drugs such as carbamazepine or phenytoin. Because the paroxysmal movements are regarded as an epileptic manifestation, paroxysmal kinesigenic dyskinesia is often misdiagnosed as epilepsy. Identification of the genes that underlie pathogenesis will enhance diagnosis and clarify the mechanisms of disease progression in paroxysmal kinesigenic dyskinesia.

Paroxysmal kinesigenic dyskinesia is most commonly transmitted in an autosomal dominant mode of inheritance[2]. Several linkage studies have identified two regions on chromosome 16 (16p11.2–q12.1 and 16q13–q22.1) that are likely to harbor paroxysmal kinesigenic dyskinesia susceptibility genes in populations of diverse ancestry[4–7]. However, sequencing of candidate genes within these regions has not led to the identification of specific pathogenesis-associated genes that account for the observed linkages[8,9].

To systematically search for paroxysmal kinesigenic dyskinesia susceptibility genes, we performed whole-exome sequencing in two affected (IV-24 and IV-25) and two unaffected (III-14 and III-21) individuals from a four-generation Han Chinese family that includes 17 individuals with paroxysmal kinesigenic dyskinesia (**Fig. 1**, family 1). The proband in our study (IV-25) is a 14-year-old boy who suffered from attacks of 'head turning to right' and 'arm spreading from the face' at age 6. Dystonic posture, which lasted for 5–10 s, was usually triggered by standing up quickly and occurred up to 10 times each day. Because of his previous diagnosis of epilepsy, he was initially treated with valproate sodium and clonazepam, which caused his symptoms to abate slightly. At age 9, this individual had a primary complaint of dyskinesia. No other abnormal physical manifestations were observed, and both electroencephalograms and magnetic resonance imaging (MRI) of the brain were normal. According to the new diagnostic criteria for paroxysmal kinesigenic dyskinesia[2], this individual was diagnosed with idiopathic paroxysmal kinesigenic dyskinesia and was prescribed 200 mg d^{-1} of carbamazepine. Seven days after treatment was started, all symptoms were improved. An additional 16 individuals in family 1 had similar symptoms. Blood samples were collected from the proband (IV-25) and from 14 other affected individuals (samples from I-1and III-15 were not available) and 20 unaffected individuals from the same family.

Exome sequencing was performed using the Agilent SureSelect Human All Exon Capture kit and 90-bp paired-end sequencing on an Illumina HiSeq 2000. An average of 4.93 billion bases of high-quality

[1]Department of Neurology and Institute of Neurology, Huashan Hospital, Institutes of Brain Science and State Key Laboratory of Medical Neurobiology, Shanghai Medical College, Fudan University, Shanghai, China. [2]Department of Neurology and Institute of Neurology, First Affiliated Hospital, Fujian Medical University, Fuzhou, China. [3]Institute of Neuroscience, State Key Laboratory of Neuroscience, Shanghai Institutes for Biological Sciences, Chinese Academy of Sciences, Shanghai, China. [4]Fudan Institute of Urology, Huashan Hospital, Shanghai Medical College, Fudan University, Shanghai, China. [5]Fudan–Van Andel Research Institute (VARI) Center for Genetic Epidemiology, School of Life Science, Fudan University, Shanghai, China. Correspondence should be addressed to Z.-Y.W. (zhiyingwu@fudan.edu.cn) or N.W. (ningwang63@yahoo.com).

Received 2 June; accepted 20 October; published online 20 November 2011; doi:10.1038/ng.1008

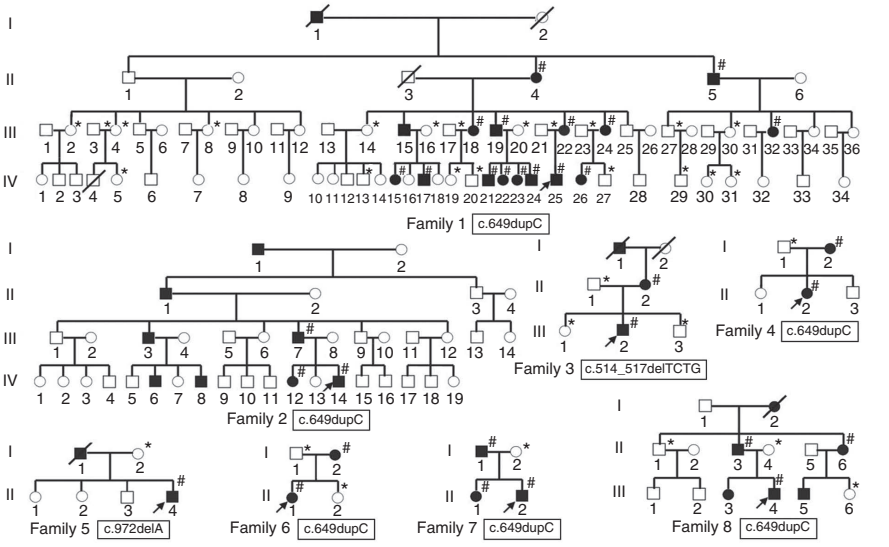

Figure 1 The pedigrees of the eight families affected by paroxysmal kinesigenic dyskinesia included in the present study. Filled-in symbols indicate individuals with paroxysmal kinesigenic dyskinesia, empty circles indicate unaffected individuals, and symbols with a slash through them indicate deceased individuals. #, affected individuals that were found to carry mutations within *PRRT2* in mutation analysis; *, unaffected individuals from whom samples were obtained for mutation analysis of *PRRT2*. Arrows indicate the probands of the families. The mutation present in *PRRT2* in each family is indicated in a box below the corresponding pedigree.

sequence was generated per individual, with 54.83% of the total bases mapped to the reference genome with a mean coverage of 72×. Sequencing data were aligned to the NCBI human reference genome (NCBI build 36.3, hg18) and compared to dbSNP129, which contains pilot data from the 1000 Genomes Project (20100208 release), from eight sequenced HapMap individuals[10] and from the YH database, which contains the first whole-genome sequence of an Asian individual[11]. An average total of 7,589 genetic variations, including non-synonymous mutations, splice-acceptor and -donor site variations, and insertions or deletions (indels), were identified per subject. These variants were then prioritized for further evaluation using two filtering criteria: if a variant was predicted to have functional impact by SIFT[12] (see URLs) and if it was found in the affected individuals but not in unaffected family members, a variant was retained for further analysis. These filtering criteria reduced the list of candidate variants to 16 non-synonymous mutations and 5 indels.

We then focused on the three candidate variants located in the paroxysmal kinesigenic dyskinesia linkage regions: an indel (chr. 16: 29732525dupC) in *PRRT2* (16p11.2), a non-synonymous mutation (chr. 16: 28511222C>T) in *SULT1A2* (16p12.1) and a non-synonymous mutation (chr. 16: 66952662T>G) in *SMPD3* (16q22.1). We first used Sanger sequencing to confirm the occurrence of these genetic variants in the same four individuals from family 1. Although we could not confirm the presence of the two non-synonymous changes, we did confirm the existence of an indel in *PRRT2*, a gene that encodes the proline-rich transmembrane protein 2. This indel causes a frameshift and the introduction of a stop codon 7 amino acids downstream of the insertion (p.Arg217Profs*8). We then used Sanger sequencing to identify this indel in samples collected from other members of family 1, including 13 individuals with paroxysmal kinesigenic dyskinesia and 18 unaffected individuals. The c.649dupC indel was found in all affected family members and was absent in all of the unaffected individuals (**Table 1**), showing complete co-segregation of the indel with paroxysmal kinesigenic dyskinesia occurrence within family 1. We also used Sanger sequencing to search for additional variants within the entire coding region of *PPRT2*, as well as within non-coding exon 1 and the intron-exon boundaries in samples collected from all the members of family 1. The primers and annealing temperature for the PCR used for this purpose are provided in **Supplementary Table 1**. No additional non-synonymous mutations, splice-acceptor or -donor site variations or indels were found within *PRRT2* in this family.

To identify additional deleterious variants in *PRRT2* among other families with a history of paroxysmal kinesigenic dyskinesia, we then performed Sanger sequencing of *PRRT2* in seven additional independent Han Chinese families that included 16 affected and 11 unaffected individuals (**Fig. 1**, families 2–8). The sequenced regions consisted of the entire length of coding exons 2–4, non-coding exon 1 and associated splice sites in *PRRT2*. The indel we identified in family 1, c.649dupC, was found in five additional families and was present in all 13 individuals with paroxysmal kinesigenic dyskinesia but in none of the 7 unaffected individuals in these families (**Fig. 1**, families 2, 4, 6, 7 and 8 and **Table 1**). Using a haplotype analysis of 36 SNPs in a 1.4-Mb region flanking the *PRRT2* gene, a common haplotype segment (189 kb) adjacent to the indel was found in three of the six families that had this genetic variant. A different haplotype segment (548 kb) was found in two other families, and a third was found in the remaining family (**Supplementary Fig. 1**). Whereas these data suggest that the indel arose independently in three different haplotype backgrounds, the possibility that it is an old founder mutation (and therefore carriers of the mutation may share a very small haplotype segment) cannot be excluded because no SNP was genotyped within the 86-kb region immediately flanking the *PRRT2* gene.

In addition to the identification of the c.649dupC indel, we found two new indels within *PRRT2* in the other families. The c.514_517delTCTG indel, which introduces a stop codon two amino acids downstream of the deletion (p.Ser172Argfs*3), was found in two individuals with paroxysmal kinesigenic dyskinesia and none of the three unaffected

Table 1 Mutations within *PRRT2* identified in subjects with paroxysmal kinesigenic dyskinesia

Family	Affected/unaffected[a]	Inheritance	Nucleotide mutation	Protein alteration	Exon
1	15/20	Transmitted	c.649dupC	p.Arg217Profs*8	2
2	3/0	Transmitted	c.649dupC	p.Arg217Profs*8	2
3	2/3	Transmitted	c.514_517delTCTG	p.Ser172Argfs*3	2
4	2/1	Transmitted	c.649dupC	p.Arg217Profs*8	2
5[b]	1/1	Unknown	c.972delA	p.Val325Serfs*12	3
6	2/2	Transmitted	c.649dupC	p.Arg217Profs*8	2
7	3/1	Transmitted	c.649dupC	p.Arg217Profs*8	2
8	3/3	Transmitted	c.649dupC	p.Arg217Profs*8	2

[a]Mutations within *PRRT2* were identified in affected individuals but not in unaffected individuals. [b]The father in this family is deceased and therefore not available for mutation analysis.

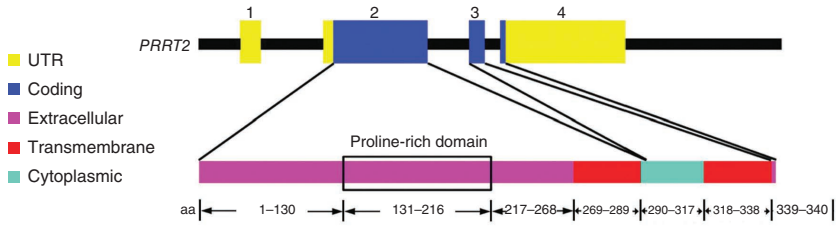

Figure 2 PRRT2 protein domain structure. The *PRRT2* gene contains four exons that encode several domains in the PRRT2 protein, including two extracellular domains, two transmembrane domains and one cytoplasmic domain. The proline-rich domain overlaps with the N-terminal extracellular domain.

family members evaluated in family 3. Another indel, c.972delA, which introduces a stop codon 12 amino acids downstream of the deletion (p.Val325Serfs*12), was found in the family member with paroxysmal kinesigenic dyskinesia and not in the unaffected family member evaluated in family 5. Chromatograms of these truncating mutations are shown in **Supplementary Figure 2**; all carriers of these indels were heterozygous for this mutation.

We performed genetic linkage analysis to assess the statistical significance of the observed co-segregation between the three indels and paroxysmal kinesigenic dyskinesia in these eight families. An autosomal dominant model was assumed, in which the disease allele frequency was set at 0.00001, and the penetrance of carriers and non-carriers was set at 0.95 and 0, respectively. The logarithm of odds (LOD) score was 7.4 in these eight families and was maximized at zero recombination fraction, suggesting that the observed complete co-segregation is unlikely to have occurred by chance.

To evaluate the frequency of these three indels in the general population, we performed Sanger sequencing on samples from 1,000 unrelated individuals of matching Han Chinese ancestry and did not find any of these indels. We then looked for additional variants within the entire coding regions, non-coding exon 1 and the intron-exon boundaries of *PRRT2* in 500 control subjects. Two known non-synonymous changes, c.412C>G (p.Pro138Arg) and c.439G>C (p.Asp147His), and five new variants were found (**Supplementary Fig. 3**). The five new alterations included three non-synonymous changes, c.640G>C (p.Ala214Pro), c.709G>A (p.Gly237Arg) and c.734G>A (p.Arg245His), and two synonymous changes, c.696C>T and c.834C>T. The non-synonymous changes were predicted to be tolerated by SIFT[12], with a SIFT score of >0.05.

PRRT2 is a poorly characterized gene. It consists of 4 exons encoding 340 amino acids, and the protein is predicted to have two transmembrane domains (involving amino acids 269–289 and 318–338) (**Fig. 2**). In a study of the expression profile of *PRRT2*, high levels of *PRRT2* mRNA were detected in many tissues of the nervous system, especially in the extrapyramidal system, which includes the globus pallidus, cerebellum, subthalamic nucleus, cerebellar peduncles and caudate nucleus[13] (see URLs). However, there are no reports of the function of the PRRT2 protein or the relationship between PRRT2 and neurological disorders.

To explore the expression pattern of *PRRT2 in vivo*, we measured the levels of *PRRT2* mRNA in various body tissues of mice by RT-PCR. At postnatal day 7 (P7), *PRRT2* was detected at low levels in the heart, lung, kidney and skin, but was most highly expressed in the brain and spinal cord (**Fig. 3a**). We then examined the temporal expression pattern of *PRRT2* in the developing mouse brain. The levels of *PRRT2* mRNA were relatively low before embryonic day 16 (E16) and were markedly increased during early postnatal stages (**Fig. 3b**). *PRRT2* mRNA levels peaked at P14 and then declined to a relatively low level in adulthood (**Fig. 3b**,**c**). We next examined the spatial distribution of *PRRT2* mRNA in the developing brain. RT-PCR and *in situ* hybridization analyses of P14 mouse brain revealed that *PRRT2* is expressed throughout the brain, with high levels present in the cerebral cortex, hippocampus and cerebellum (**Fig. 3d–f**), and expression is enriched in cortical layers of the cerebral cortex, as well as in granule cells and Purkinje cell layers of the cerebellum (**Fig. 3f**). To examine the subcellular localization of the PRRT2 protein and test whether the truncation of PRRT2 affects its subcellular localization, we generated constructs encoding GFP-tagged wild-type (WT PRRT2-GFP) and truncated (amino acids 1–230; Δc PRRT2-GFP) PRRT2 (**Fig. 4a**). The membrane localization of WT PRRT2-GFP was confirmed in COS-7 cells (**Fig. 4b**, left). Of note, Δc PRRT2-GFP lost membrane targeting and was located in the cytoplasm (**Fig. 4b**, right).

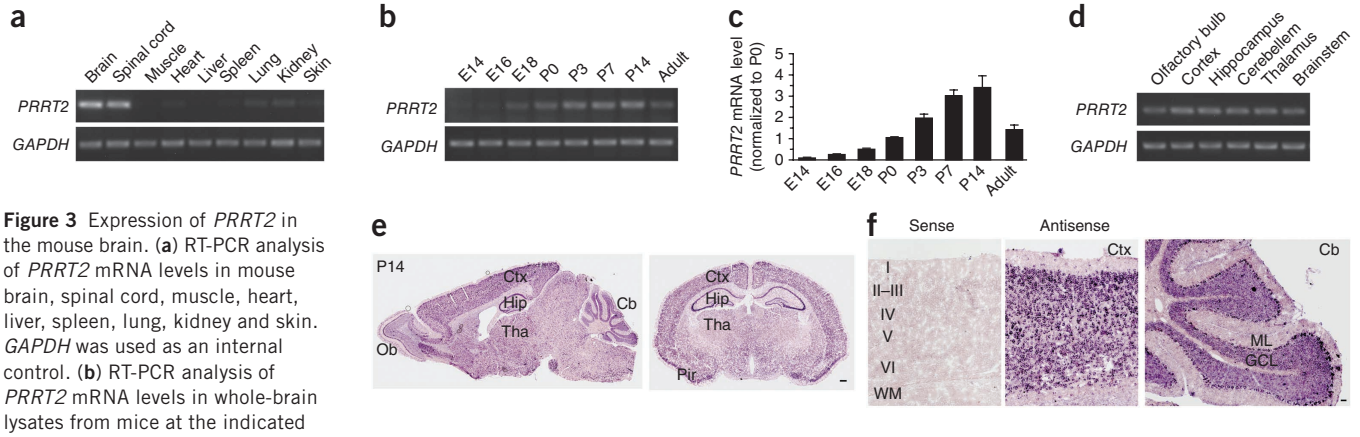

Figure 3 Expression of *PRRT2* in the mouse brain. (**a**) RT-PCR analysis of *PRRT2* mRNA levels in mouse brain, spinal cord, muscle, heart, liver, spleen, lung, kidney and skin. *GAPDH* was used as an internal control. (**b**) RT-PCR analysis of *PRRT2* mRNA levels in whole-brain lysates from mice at the indicated stages of development. (**c**) *PRRT2* mRNA levels in the developing mouse brain ($N = 4$ at each time point) determined by qPCR and normalized to the levels in P0 mice. Error bars represent s.e.m. (**d**) RT-PCR analysis of *PRRT2* mRNA levels in the different brain regions. (**e**,**f**) *In situ* hybridization (ISH) for *PRRT2* in the P14 mouse brain. Ctx, cortex; Ob, olfactory bulb; Cb, cerebellum; Tha, thalamus; Hip, hippocampus; Pir, piriform cortex; ML, molecular layer; GCL, granule cell layer; WM, white matter. Roman numerals (I–VI) indicate layers of the cerebral cortex. ISH with sense probe served as a negative control. Scale bars, 300 μm in **e**, 30 μm in **f**.

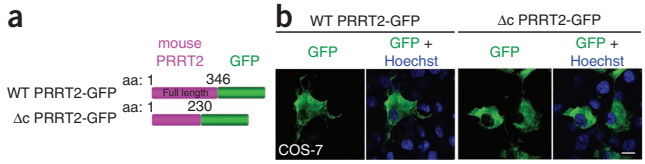

Figure 4 Truncated PPRT2 has altered cellular localization. (**a**) Schematic diagrams of the protein structure of wild-type PRRT2 fused to GFP (WT PRRT2-GFP) and of a truncated form of PRRT2 fused to GFP (Δc PRRT2-GFP). (**b**) Representative images showing the localization of WT PRRT2-GFP (left) and Δc PRRT2-GFP (right) in COS-7 cells. Scale bar, 10 μm.

Taken together, these results indicate that *PRRT2* is highly expressed in the developing nervous system and that truncating mutation results in altered subcellular localization of the protein.

Considering that paroxysmal kinesigenic dyskinesia is a paroxysmal neurologic disorder and that ion-channel blockers such as carbamazepine are highly effective at a low dose, it has been proposed that paroxysmal kinesigenic dyskinesia is an ionic channelopathy[14,15]. As a transmembrane protein, PRRT2 may form a complex with an ion channel or regulate key properties of ion channels related to paroxysmal kinesigenic dyskinesia. Two indels described in this study, c.649dupC (p.Arg217Profs*8) and c.514_517delTCTG (p.Ser172Argfs*3), are located within the segment of the gene encoding the proline-rich domain, and both overlap with the N-terminal extracellular domain. Therefore, the resulting truncated proteins may completely lose their transmembrane function. The c.972delA (p.Val325Serfs*12) mutation is located in the second transmembrane motif and thus may also interrupt transmembrane domain integrity and function. Furthermore, these truncating mutations are all predicted to influence the function of specific types of ion channels and may thereby give rise to paroxysmal kinesigenic dyskinesia. However, the function of PRRT2 and its role in paroxysmal kinesigenic dyskinesia should be further investigated in future studies.

In summary, we have identified three highly penetrant truncating mutations in the *PRRT2* gene. This identification of the first gene to be associated with paroxysmal kinesigenic dyskinesia pathogenesis has the potential to improve the understanding of the molecular basis of this disease. With additional research, this finding may also lead to improved clinical diagnosis and treatment for paroxysmal kinesigenic dyskinesia.

URLs. Prevalence of paroxysmal kinesigenic dyskinesia, http://www.ncbi.nlm.nih.gov/books/NBK1460/; SIFT, http://sift.jcvi.org/; Expression profile of *PRRT2*, http://www.ebi.ac.uk/gxa/experiment/E-AFMX-5/ENSG00000167371.

Accession numbers. The sequence of human *PRRT2* has been deposited at Ensembl (ENSG00000167371). The expression data for PRRT2 are available from the ArrayExpress web-based tool (ENSG00000167371).

METHODS

Methods and any associated references are available in the online version of the paper at http://www.nature.com/naturegenetics/.

Note: Supplementary information is available on the Nature Genetics website.

ACKNOWLEDGMENTS

The authors sincerely thank the participants for their help and willingness to take part in this study. The authors also thank the Beijing Genomics Institute (BGI)-Shenzhen for assistance in the analysis of exome sequence data. This work was supported by a grant from the National Natural Science Foundation (China; 81125009 to Z.-Y.W.) and a grant from Huashan Hospital for the special professorship of Fudan University (to Z.-Y.W.) and by a key program of scientific research of Fujian Medical University (2009D064 to N.W.).

AUTHOR CONTRIBUTIONS

N.W. and Z.-Y.W. planned the project. Z.-Q.X., J.X., N.W. and Z.-Y.W. conceived of and designed the study. W.-J.C., Yu Lin, Yi Lin, S.-X.M., N.W. and Z.-Y.W. performed the sample collection. W.-J.C., Yu Lin, W.W., W.N., J.H., Y.-F.C., Q.-J.Z. and H.-F.L. performed sequence analysis. J.-F.X. and Z.-Y.W. performed linkage and haplotype analyses. Z.-Q.X., G.-H.T. and S.-L.G. performed the expression analysis. W.-J.C., Z.-Q.X., J.X., N.W. and Z.-Y.W. analyzed the data. W.-J.C., Z.-Q.X. and Z.-Y.W. wrote the manuscript, and J.X. and Z.-Y.W. revised it.

COMPETING FINANCIAL INTERESTS

The authors declare no competing financial interests.

Published online at http://www.nature.com/naturegenetics/.
Reprints and permissions information is available online at http://www.nature.com/reprints/index.html.

1. Kertesz, A. Paroxysmal kinesigenic choreoathetosis. An entity within the paroxysmal choreoathetosis syndrome. Description of 10 cases, including 1 autopsied. *Neurology* **17**, 680–690 (1967).
2. Bruno, M.K. *et al.* Clinical evaluation of idiopathic paroxysmal kinesigenic dyskinesia: new diagnostic criteria. *Neurology* **63**, 2280–2287 (2004).
3. Goodenough, D.J., Fariello, R.G., Annis, B.L. & Chun, R.W. Familial and acquired paroxysmal dyskinesias. A proposed classification with delineation of clinical features. *Arch. Neurol.* **35**, 827–831 (1978).
4. Tomita, H. *et al.* Paroxysmal kinesigenic choreoathetosis locus maps to chromosome 16p11.2-q12.1. *Am. J. Hum. Genet.* **65**, 1688–1697 (1999).
5. Swoboda, K.J. *et al.* Paroxysmal kinesigenic dyskinesia and infantile convulsions: clinical and linkage studies. *Neurology* **55**, 224–230 (2000).
6. Bennett, L.B., Roach, E.S. & Bowcock, A.M. A locus for paroxysmal kinesigenic dyskinesia maps to human chromosome 16. *Neurology* **54**, 125–130 (2000).
7. Valente, E.M. *et al.* A second paroxysmal kinesigenic choreoathetosis locus (*EKD2*) mapping on 16q13-q22.1 indicates a family of genes which give rise to paroxysmal disorders on human chromosome 16. *Brain* **123**, 2040–2045 (2000).
8. Kikuchi, T. *et al.* Paroxysmal kinesigenic choreoathetosis (PKC): confirmation of linkage to 16p11-q21, but unsuccessful detection of mutations among 157 genes at the PKC-critical region in seven PKC families. *J. Hum. Genet.* **52**, 334–341 (2007).
9. Ono, S. *et al.* Mutation and copy number analysis in paroxysmal kinesigenic dyskinesia families. *Mov. Disord.* **26**, 761–763 (2011).
10. Ng, S.B. *et al.* Targeted capture and massively parallel sequencing of 12 human exomes. *Nature* **461**, 272–276 (2009).
11. Wang, J. *et al.* The diploid genome sequence of an Asian individual. *Nature* **456**, 60–65 (2008).
12. Ng, P.C. & Henikoff, S. SIFT: predicting amino acid changes that affect protein function. *Nucleic Acids Res.* **31**, 3812–3814 (2003).
13. Su, A.I. *et al.* A gene atlas of the mouse and human protein-encoding transcriptomes. *Proc. Natl. Acad. Sci. USA* **101**, 6062–6067 (2004).
14. Bhatia, K.P., Griggs, R.C. & Ptácek, L.J. Episodic movement disorders as channelopathies. *Mov. Disord.* **15**, 429–433 (2000).
15. Celesia, G.G. Disorders of membrane channels or channelopathies. *Clin. Neurophysiol.* **112**, 2–18 (2001).

ONLINE METHODS

Subjects and samples. The clinical data and blood samples were obtained from eight Chinese Han families with paroxysmal kinesigenic dyskinesia that included 31 affected and 31 unaffected individuals; all individuals with paroxysmal kinesigenic dyskinesia met the new diagnostic criteria for the disease. Two affected individuals and two unaffected individuals from family 1 were selected for whole-exome sequencing, and the remaining individuals and 1,000 controls of matched ancestry were recruited for Sanger sequencing. This study was approved by the ethics committee of the First Affiliated Hospital of Fujian Medical University, and written consent was obtained from all participants or their guardians.

Whole-exome sequencing. Genomic DNA was extracted from peripheral blood using a QIAamp DNA Blood Mini kit (Qiagen). Genomic DNA (3 μg) was randomly fragmented by Covaris, and the resulting fragments were ligated with adaptors (Illumina). After purification using Agencourt AMPure SPRI beads (Beckman Coulter Genomics), the adaptor-ligated templates were amplified by ligation-mediated PCR (LM-PCR) and hybridized to the SureSelect Biotinylated RNA Library (BAITSl Agilent) for enrichment. Each captured library was then loaded onto the HiSeq 2000 sequencing platform to ensure that each sample was covered to a depth of at least 20×. Raw image files were processed using Illumina Pipeline version 1.6 for base calling with default parameters, and the sequences of each individual were generated as 90-bp paired-end reads. SOAPaligner (SOAP2.20)[16] was used to align the clean reads to the NCBI human reference genome (NCBI build 36.3). On the basis of SOAP alignment results, SOAPsnp software[17] was used to assemble the consensus sequence and call genotypes in target regions. Insertions and deletions (indels) in the exome regions were identified using GATK[18]. Public data available from dbSNP129, the 1000 Genomes Project, HapMap 8 and the YH database were used for analysis of the results.

Sanger sequencing. Sanger sequencing was performed to confirm the variants found by whole-exome sequencing and to search for additional variants. The PCR primers (sequences provided in **Supplementary Table 1**) were designed to amplify the entire exons and the intron-exon boundaries of *PRRT2*. PCR amplification was carried out using a GeneAmp PCR System 9700 (Applied Biosystems) using standard conditions. PCR products were purified in a 5-μl volume containing 0.08 μg of the amplified product, 0.3 units of shrimp alkaline phosphatase (Promega) and 4 units of exonuclease I (New England Biolabs) for one cycle of 60 min at 37 °C and 15 min at 80 °C. The purified PCR products were sequenced with an ABI PRISM BigDye Terminator Cycle Sequencing Ready Reaction kit (Applied Biosystems) using standard conditions. The sequencing products were purified by ethanol/EDTA/sodium acetate precipitation and analyzed on an ABI 3730 Automated DNA Sequencer (Applied Biosystems). The sequences we obtained were compared with the genomic DNA sequence of *PRRT2*, and nucleotide changes were numbered corresponding to their position in *PRRT2* mRNA (Ensembl gene ID: ENSG00000167371).

Genetic linkage analysis. Linkage analyses were performed using GENEHUNTER software[19]. An autosomal dominant model was assumed, and the disease allele frequency was set at 0.00001 to reflect the occurrence rate of 1 in 150,000. The penetrance of carriers and non-carriers was set at 0.95 and 0, respectively. This model was based on an assumption of a highly penetrant paroxysmal kinesigenic dyskinesia mutation with no phenocopy.

Haplotype analysis. Haplotype analysis was performed for 36 SNPs in a 1.4-Mb region flanking the *PRRT2* gene using GENEHUNTER[19]. The most likely haplotypes of each subject were inferred using a maximum-likelihood method based on multipoint inheritance in families.

Real-time PCR and qPCR. Brain tissue from C57BL/6 mice was quickly dissected on ice and homogenized in TRIzol Reagent (Invitrogen) at 4 °C. RNA was extracted and reverse transcribed with MMLV reverse transcriptase (Invitrogen). PCR amplification was performed in a final volume of 20 μl. The primers used are listed in **Supplementary Table 2**. PCR products were analyzed on 1% agarose gels. Real-time PCR analysis of *PRRT2* expression was performed using SYBR Premix Ex Taq (Takara) in an ABI PRISM 7000 thermal cycler, according to the manufacturer's instructions. Dissociation curve analysis was carried out after PCR amplification to confirm the absence of non-specific amplification products and primer dimers.

***In situ* hybridization.** *In situ* hybridization was performed as previously described[20]. Briefly, C57BL/6 mice were deeply anesthetized and perfused with 4% paraformaldehyde (PFA) in 0.1 M PBS (DEPC-PBS; pH 7.4). Whole brains were removed and placed into 4% PFA in DEPC-PBS for 12–16 h at 4 °C and then dehydrated in a sucrose gradient (15–30%) dissolved in DEPC-PBS. Coronal brain sections (20 μm) were cut with a Cryostat (CM1900, Leica) and mounted onto RNase-free, saline-coated slides (Fisher Scientific). RT-PCR products for mouse *PRRT2* (nucleotides 308–1189; NM-001102563) were inserted into the pGEM-T Easy vector (Promega). Digoxigenin-labeled antisense and sense (control) riboprobes were then synthesized from linearized plasmids using the DIG RNA labeling kit (Roche). Hybridization was performed following the standard protocol and was detected with the nitro blue terazolium/5-bromo-4-chloro-3-indolyl phosphate (NBT/BCIP) system (Boehringer Mannheim). Images were acquired with a Nikon E600FN upright microscope using Neurolucida software.

Construct preparation, cell culture, transfection and imaging. Mouse *PRRT2* sequence was amplified by RT-PCR from a cDNA library of mouse brain. PCR products encoding full-length (amino acid 1–346) or truncated (amino acids 1–230) mouse PRRT2 were cloned into pCAG-EGFP-N1 (Clontech) at EcoRI and AgeI sites using the In-Fusion PCR Cloning System (Clontech) and were verified by sequencing. The primers for the amplification of these sequences are provided in **Supplementary Table 2**. COS-7 cells were cultured in DMEM (Invitrogen) supplemented with 10% fetal bovine serum (FBS) and were transfected with Lipofectamine 2000 (Invitrogen) according to the manufacturer's instructions. Cells were fixed in 4% PFA-PBS with 4% sucrose 48 h after transfection and mounted with DAKO mounting medium. GFP-positive cells were imaged with the Nikon Eclipse FN1 confocal microscope under a 60x oil objective with numerical aperture of 1.4. Images were processed with ND2 viewer and ImageJ software.

16. Li, R. *et al.* SOAP2: an improved ultrafast tool for short read alignment. *Bioinformatics* **25**, 1966–1967 (2009).
17. Li, R. *et al.* SNP detection for massively parallel whole-genome resequencing. *Genome Res.* **19**, 1124–1132 (2009).
18. McKenna, A. *et al.* The genome analysis toolkit: a MapReduce framework for analyzing next-generation DNA sequencing data. *Genome Res.* **20**, 1297–1303 (2010).
19. Kruglyak, L., Daly, M.J., Reeve-Daly, M.P. & Lander, E.S. Parametric and nonparametric linkage analysis: a unified multipoint approach. *Am. J. Hum. Genet.* **58**, 1347–1363 (1996).
20. Hu, X.L. *et al.* Conditional deletion of NRSF in forebrain neurons accelerates epileptogenesis in the kindling model. *Cereb. Cortex* **21**, 2158–2165 (2011).

doi:10.1038/ng.1008